

# Computational study of flow over Fire II Re-entry Vehicle at various Supersonic Speeds

Kanishka Deepak<sup>1</sup>, Anish G P Nand<sup>2</sup>

<sup>1</sup> Aerospace Engineering, R V College of Engineering, Bengaluru, India

<sup>2</sup> Aerospace Engineering, R V College of Engineering, Bengaluru, India

## ABSTRACT

*Abstract: Re-entry modules are blunt bodies that are designed in such a way that they can withstand the extreme temperature loads during atmospheric re-entry. Designing a re-entry vehicle requires dependable data on the aerodynamic flow properties. After hypersonic re-entry, the vehicle has to decelerate at supersonic speeds until the parachutes are deployed. Examining the flow properties over the vehicle at supersonic speed is important of which temperature serves as critical data for a successful recovery operation. Hence this paper is presented to understand the variation in temperature, as the re-entry vehicle decelerates from Mach no. 3 to 1.2. Temperature variation along with pressure distribution is obtained computationally for freestream Mach numbers 1.2, 2 and 3 with appropriate boundary conditions using Ansys FLUENT. The results also describe the flow field around a capsule in supersonic flow and understand the importance of shock waves which influences the aerodynamic forces on the capsule. The analysis showed the flow-field features such as bow shock wave on the frontal heat shield surface and expansion fan on the shoulder terminating region around the re-entry capsule. This research will assist spacecraft design engineers to analyse the flowfield and choose the appropriate materials. Further, the analysis performed can aid in the designing of parachutes that are used to decelerate the re-entry vehicle for a safe landing.*

**Keyword:** - Re-entry vehicle, capsule, Supersonic flow, Computational fluid dynamics, Thermal heating, Heat flux, Shock waves, Ansys.

## 1. INTRODUCTION

Meteors that enter the atmosphere from space burn up at extremes of temperatures and vaporize. Therefore, for a vehicle to return back to earth after its completion of the space mission, various methods are used to slow down the vehicle and reduce the temperature. Re-entry vehicles are blunt bodies that generate high aerodynamic during atmospheric re-entry. It has a reduced vehicle dimension for minimizing the total structural weight and based on the type of trajectory, the ballistic and lifting-body coefficient is chosen.

The re-entry vehicle shape used in the mercury project as shown in Fig.1 was blunt shape capsules which were designed with a thermal protection system to protect the aerodynamic heating during re-entry. After re-entry, a parachute was deployed to safely land on the seawater [1]. The parachutes are only deployed once the vehicle reaches subsonic velocities. Therefore, examining flow over the re-entry vehicle at supersonic speeds serves as a piece of critical information to design adequate thermal systems for the vehicle.

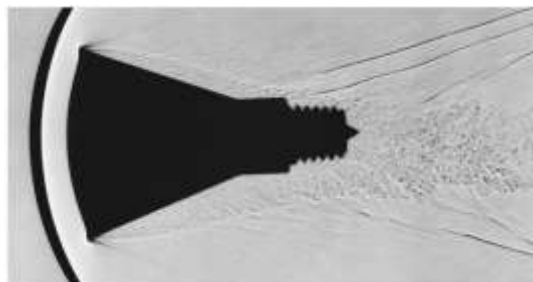


**Fig-1** Separated flow on smooth-faced Mercury capsule at Mach 3.28 and 2.0 deg AOA[1].

In this paper, the aerothermodynamic properties such as pressure and temperature over the re-entry vehicle are computed for various Mach numbers. The Re-entry vehicle chosen for the simulation is the Fire-II Model which was an experiment to determine the high-temperature regions during atmospheric entry at lunar return speeds.

## 2. LITERATURE REVIEW

### 2.1 Aerothermal Analysis

The study by Michael Wright et. al.[2] involved in simulating the wake flow and afterbody heating environment of the Project Fire II flight experiment using computational fluid dynamics. The results obtained over the first portion of the trajectory, spanning the period from the onset of significant afterbody heating to the peak heating point. By computing heat transfer on the conical frustum portion of the afterbody it was compared to the flight data.

This analysis pointed to the possibility that catalysis was occurring on the after-body heat shield. Computations were then made assuming both a fully catalytic afterbody surface and a partially catalytic surface using a material model for SIRCA, which was chosen to approximate the catalytic properties of the surface coating prior to the onset of pyrolysis. The computations including finite-rate catalysis, particularly the SIRCA model, are in good agreement with the data over the early portion of the trajectory. Comparing the computations and flight data from Fire II with previous data suggests that another mechanism, possibly pyrolysis, may be occurring during this portion of the flight, reducing the total heat transfer over the predictions that do not include material response.

### 2.2 Aeroheating of a Titan Probe

Olejniczak et. al.[3], work presents the convective and radiative aero heating results for the afterbody of a candidate aerocapture vehicle for Titan. It is shown that the afterbody aero heating environment for a Titan aerocapture vehicle is dominated by radiation from the CN radical formed in the nonequilibrium shock layer. Considering the undershoot design trajectory using the minimum atmosphere model, convective heating rates are usually less than 1 w/cm<sup>2</sup> on the whole afterbody, while the radiative heating rates on large areas of the afterbody are up to 7 ~w/cm<sup>2</sup>. Radiative heating rates at the shoulders are up to 20 ~w/cm<sup>2</sup>, compared to a maximum convective heating of 6 ~w/cm<sup>2</sup>. It can be concluded that the radiation-flow field coupling removes energy from the flow field and reduces both the convective and radiative heating on the afterbody by 25 to 70%, depending on the specific surface location and time along the trajectory.

### 2.3 Eddy Simulation of Hypersonic Flows with its Application

The investigation conducted by Sinha et. al.[4] describes the afterbody flow field on the Fire II vehicle and the proposed Titan probe using detached eddy simulation involving three-dimensional multi-block grids. The grid in the base region was designed to capture the unsteady wake. The flow in the large recirculation region on the Fire II afterbody was found to be highly unsteady with a large range of length scales. The high degree of three-dimensionality results in localized high heat transfer rate to the vehicle. The turbulent mixing in the flow also results in higher flow-field temperature than a laminar simulation. This leads to a higher heat transfer rate to the afterbody in the turbulent simulation. However, the afterbody pressure in the turbulent case was lower than the laminar flow.

### 2.4 Space Shuttle Reentry

The CFD analysis by Likhith Nallur et. al.[5] showed that blunt shock waves are preferred over oblique shock waves because the oblique shock waves increase the effects of parameters like velocity, temperature, and pressure on the surface of the Reentry capsule compared to blunt shock waves. Due to an increase in the parameters, the heat transfers through the capsule increasingly and thereby damages the foam under the thermal shield which is extremely dangerous for the capsule. Hence most of the space vehicles which are reentering the earth's atmosphere are designed in the shape of blunt profile to reduce the effect of forming oblique shock which will be dangerous for the capsule.

### 3.METHODOLOGY

The steps involved in the CFD analysis of a Fire II Re-entry vehicle in Ansys FLUENT have been discussed briefly:(i). The geometry of Fire II is defined (ii). The designed model is imported and meshed (iii). An appropriate solver and equation is selected (iv). The boundary conditions were defined for each case (v). The convergence criteria were set to the order of  $10^{-6}$  for continuity x, y and z velocities, energy calculation and turbulence quantities  $k$  and  $\omega$  for accurate results (vi). Post-processing the output and evaluating the results.

#### 3.1 Geometry

Figure 2, shows a schematic of the Fire II vehicle [2]. The spherical forebody consisted of a multi-layer configuration made of three protective phenolic asbestos heat shields sandwiched between three beryllium calorimeters. The initial two calorimeters and their related heat shields were discharged during the flight at predetermined deceleration loads. The later part shape of the re-entry, which is given by ejection of the third heat shield, is of importance in this work. The afterbody is conical with a  $66^\circ$  included angle. The C-band antenna which is situated at the base is switched by a flat base to make it simpler, which gives the geometry of the vehicle used in the current work.

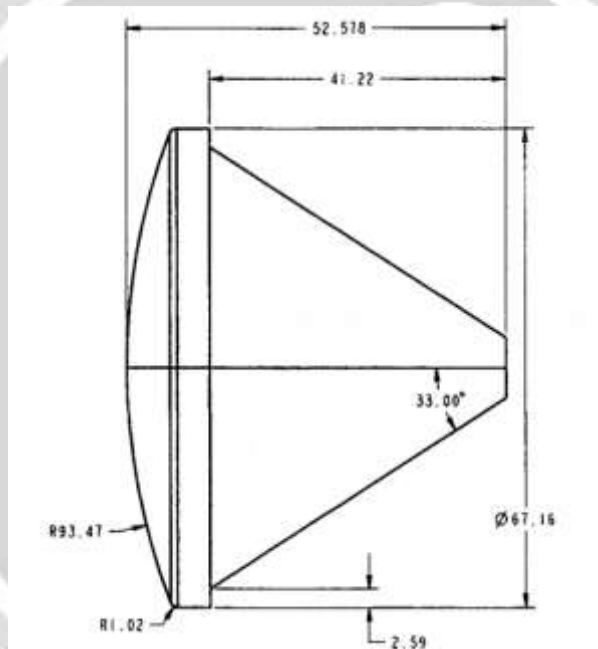


**Fig-2** Relevant dimensions (in centimeters) of the Fire II reentry Vehicle [2]

#### 3.2 Fire II Fluid Domain Modelling

The re-entry vehicle and fluid domain are modelled on SpaceClaim, a built-in Ansys Design workbench. The far-field is modelled around the body to create an environment that replicates an experimental section to account for the fact that air flows around the Re-entry vehicle. Fig. shows the two dimensional CFD domain where the Re-entry vehicle is solid and the far-field is the fluid domain. The Fluid is considered an Ideal gas around the body [6]. The flow field around the re-entry body is simulated by resolving the three-dimensional Navier- Stokes equations. Fig.3 shows the two-dimensional atmospheric far-field with the capsule. The domain is modelled as factors of the Fire-II re-entry vehicle dimensions in order to form a high-quality mesh around the heat shield.

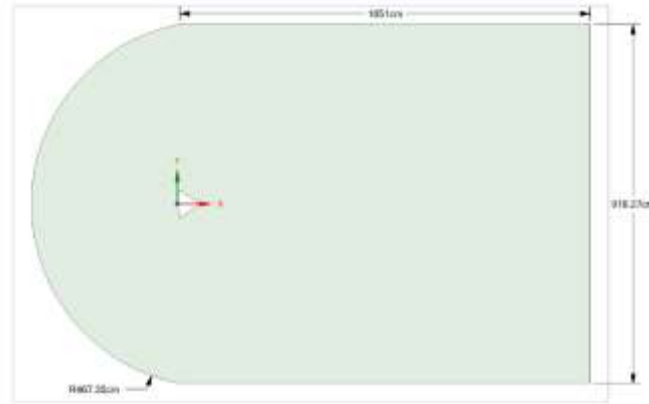


**Fig-3** Two dimensional CFD domain

### 3.3 Meshing

The mesh model is created to simulate the supersonic flow over the Fire-II Re-entry vehicle. The domains are split about the geometry of the re-entry model as shown in Fig.4(a) to form a structured mesh. The fluid domain is meshed with the multi-zone quadrilateral elements. The final mesh consisted of 50582 elements and 50998 nodes. The obtained mesh has an average Aspect ratio of 1.0755 and an Orthogonal quality of 0.995.

Quality of the mesh decides one of the controlling factors of the flow simulation around the body. As seen in Fig.4(b)(c), the grid is uniformly refined in the region of the shock wave to accurately capture the flow gradients. Note that meshing near the heat shield is most fine and accurate. The meshed file is imported into ANSYS FLUENT where suitable boundary conditions and operating conditions are given to get all the performance parameters during the supersonic re-entry.

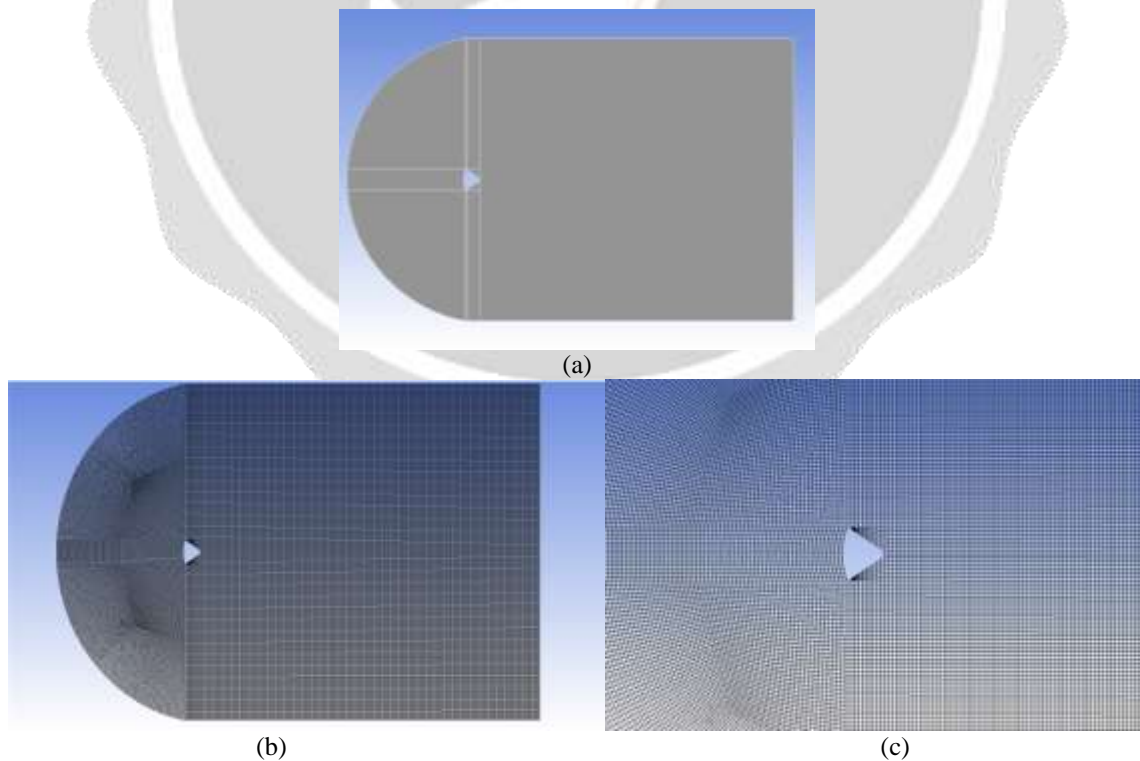


**Fig-4** Mesh model

### 3.4 Turbulence Model

Turbulent flows are characterised by means of fluctuating velocity fields. These variations blend transported quantities such as momentum, energy, and species concentration, and cause the transported quantities to fluctuate as well. Since these variables can be of limited scale and high frequency, they are excessively computationally expensive to simulate straightforwardly in practical engineering calculations. Instead, the instantaneous (exact) governing equations can be time-averaged, ensemble-averaged, or otherwise manipulated to remove the small scales, resulting in a modified set of equations that are computationally affordable to solve. Nonetheless, the modified equations contain additional unknown variables, and turbulence models are expected to determine these variables in terms of known quantities [7].

The k- $\epsilon$  turbulence model is a two-equation model wherein the solution of two separate transport equations lets the turbulent velocity and length scale be independently determined. Robustness, economy, and sensible accuracy for a wide scope of turbulent flows explain its modern stream in industrial flow and heat transfer simulations. The standard k- $\epsilon$  model is a semi-empirical model which is dependent on model transport equations for the turbulence kinetic energy (k) as well as its dissipation rate ( $\epsilon$ ). The model transport equation for k is obtained from the accurate equation, whilst the model transport equation for  $\epsilon$  was acquired using physical reasoning and carries similarity to its mathematically exact counterpart [8]. The k- $\epsilon$  model is utilized in the present paper to validate the turbulent flow over reentry bodies.

### 3.5 Boundary conditions

The free-flight experiment examines the influence of physical phenomena on the wall heat distribution along the re-entry trajectory [9]. Viscous shock layer (VSL) and Navier–Stokes (NS) solutions were created for chosen trajectory points with various levels of modelization, where at the wall, a temperature distribution was recommended [10].

The appropriate boundary conditions and operating conditions are given to get all the performance parameters during the re-entering into the earth atmosphere. The freestream conditions for each case are enumerated in Table 1, which are used as the initial conditions. Freestream value is represented by the subscript  $\infty$  in Table 1. They are prescribed as follows:

**Table-1** Initial conditions

$M_\infty$	$P_\infty$ (Pa)	$T_\infty$ (K)
1.2	4519	210
2.0	2891	219
3.0	2073	224

### 3.6 Simulation

The execution of the simulation is performed by the Ansys FLUENT program, where the simulation is done on four processors (in parallel). A steady-state solver was formulated and equations were solved (turbulent), material properties, specification of operating and boundary conditions, specification of numerical properties was performed. The flow field around the Fire II Re-entry body is initialized to free-stream values all over the domain. The residuals were tracked in the interface window of the FLUENT workbench. For all the cases, iterations continued till the convergence ( $10^{-6}$ ) or near convergence were reached.

### 4. RESULTS AND DISCUSSION

The simulation of the Fire-II vehicle is performed for three Mach numbers as shown in Table-1. As the simulation progresses, shock and the boundary layer on the vehicle are formed, followed by flow separation on the aft of the re-entry vehicle. In this section, the effect of supersonic flow on the vehicle is discussed. It is done with respect to velocity, pressure, and temperature distribution around the body. The temperature distribution at the vehicle surface is also discussed.

#### 4.1 Velocity Profile

As seen in Fig 5, the velocity at the heat shield tends to approach zero and forms the stagnation region. However, the velocity distribution over the re-entry varies as it decelerates from Mach 3 to Mach 1.2. The Mach number behind the bow shock wave formed in front of the vehicle tends to reduce with decreasing freestream Mach number. This effect is seen with increasing stand-off distance between the heat shield and the bow shock. The shock expansion waves over the model shoulder can be visualized in the form of a high flow velocity region. The flow in this region tends to get complicated upon dissipation at a lower Mach number, as seen in Fig 5(a).

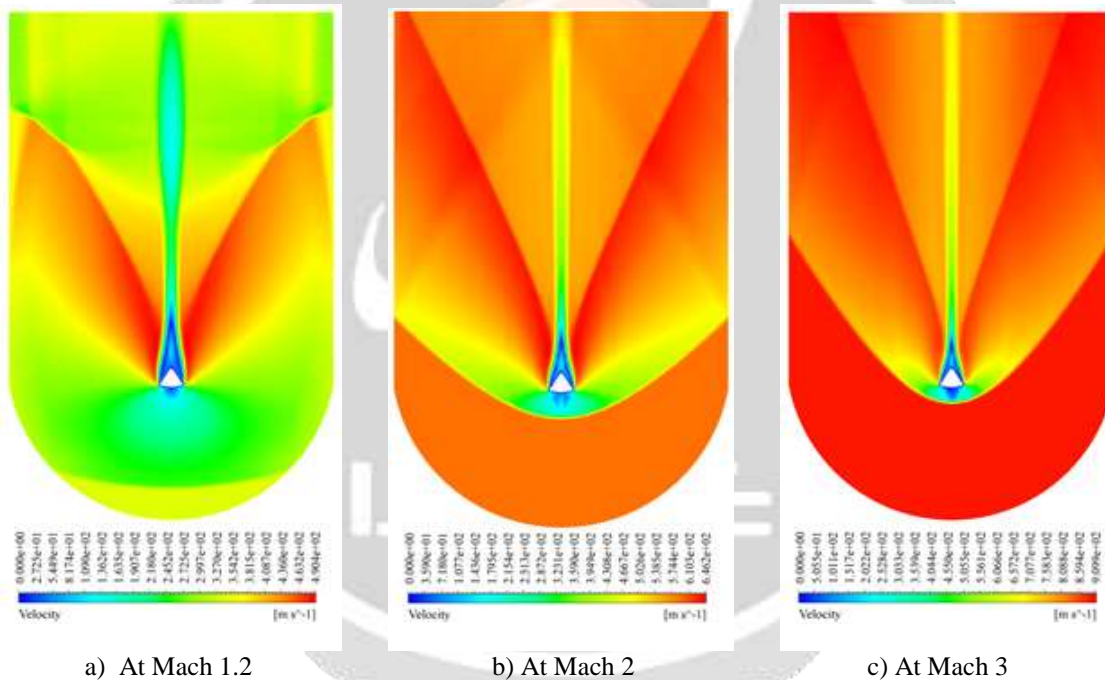


Fig-5 Velocity contour plot over Fire II Re-entry Vehicle

#### 4.2 Pressure Profile

During re-entry, there are strong bow shock waves generated on the frontal region of the vehicle. This region as seen in Fig 6 is characterized by maximum pressure. At the shoulders of the vehicle, the pressure tends to dissipate due to the formation of expansion waves. Due to the presence of the bow shock, there is a high drag force that exerts on the vehicle which decelerates it to a lower Mach number. The pressure variations as shown in Fig 6 suggest the same. As Mach number increases, the strength of the shock also increases which results in an increase in curvature of it around the vehicle corner.



### 4.4 Local Temperature over FIRE-II

The temperature is plotted on the re-entry vehicle to understand the heat distribution over it. This analysis allows designers to choose the appropriate material for the heat shield as well as other parts of the body. As inferred from Fig. 7, the temperature is maximum at the front end of the vehicle. As the Mach number increases the temperature also increases which results in an increase in the heat flux over the capsule. The temperature variations also depend on the standoff distance of the bow shock wave as well as the pressure distribution over the entire re-entry vehicle. It can be seen that due to narrow near neck flow at a high Mach number, the temperature is high. Therefore, the material of the vehicle can be varied based on the different heat zones.

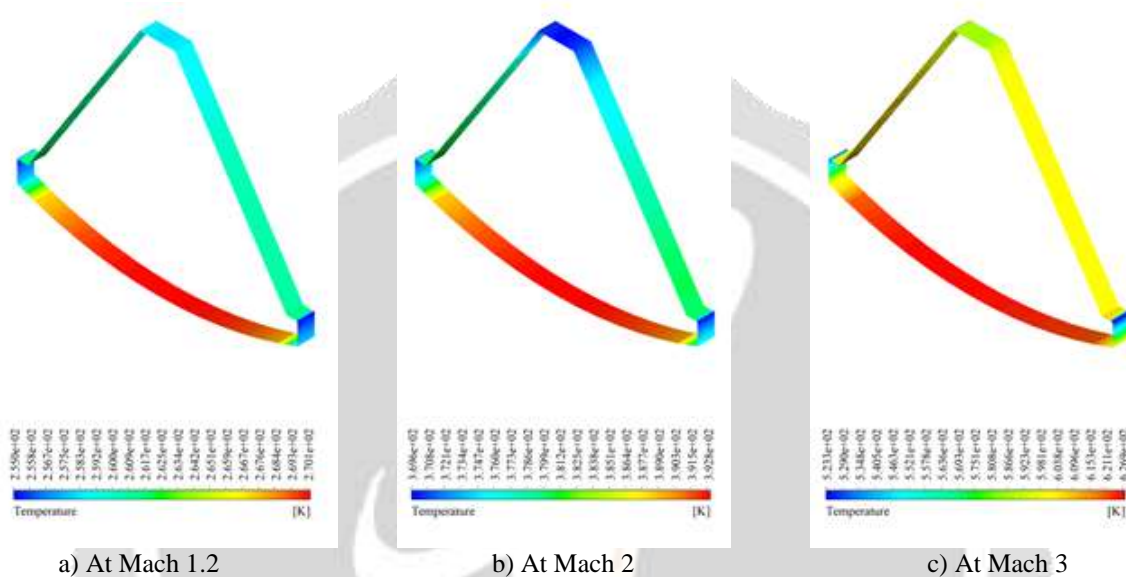


Fig-8 Temperature variation across Fire II Re-entry Vehicle

The maximum and minimum temperature and pressure are tabulated in table 2 at their respective Mach numbers.

Table-2 Temperature and Pressure for various Mach numbers

Mach Number	Temperature ( K )		Pressure ( Pa )		Temperature over Vehicle ( K )	
	Minimum	Maximum	Minimum	Maximum	Minimum	Maximum
1.2	149.6	269.6	-3.255e+03	6.224e+03	2.550e+02	2.701e+02
2	184.2	392.0	-1.915e+03	1.375e+04	3.696e+02	3.928e+02
3	210.6	628.7	-1.274e+03	2.131e+04	5.233e+02	6.269e+02

### 5. CONCLUSION

The flow field around the Fire II re-entry module is computed for various Mach numbers to study various parameters like velocity, pressure and temperature along with the heat flux on the surface of the module using two-equation k - ω models for turbulence closure. At supersonic speeds, the characteristic flow features around the blunt-body are visualised where the shock wave formed comes closer to the body with an increase in Mach number. Thus, the FIRE II re-entry vehicle is analyzed while decelerating from Mach number 3 to 1.2. It can be observed that the velocity at the heat shield is minimum and increases as we move to the shoulder. This decrease in velocity results in

an increase in pressure gradient which results in the formation of a shock wave. At Mach number 1.2 the velocity over the body is twice as that observed for Mach 3.

The high surface pressure develops larger aerodynamic drag on the fore-body which is essential for atmospheric aerobraking. It is observed that the pressure at Mach 1.2 is 3.7 times less compared to the pressure around the body entering at Mach 3. Due to viscous force and high-pressure force, it experiences the high-temperature distribution to the fluid and also to the capsule. The temperature of the flow around the body while reentering at Mach 3 is 2.31 times more as compared to body re-entering at Mach 1.2.

Surface wall temperature obtained from the aerothermal analysis helps us choose material for the survival of the vehicle hence heat transfer is computed on the conical frustum portion of the afterbody and was compared for different Mach number. This analysis gives the idea of heat distribution around the re-entry capsule body at different Mach numbers. As the Mach number increases the temperature also increases due to friction. Localised heating can be avoided by the right choice of material. The investigation proves that this approach further provides aerodynamic parameters to validate numerical methods and commercial experimenting methods on a timely basis while keeping the cost. The method shows how it makes the research on reentry much easier than it was before.

## 6. REFERENCES

- [1]. L Robert, O Neal and Leonard Rabb. Heatshield performance during atmospheric Entry of project mercury Research and Development Vehicle NASA. May 1961
- [2]. Wright, Michael & Loomis, Mark & Papadopoulos, Periklis. (2003). Aerothermal Analysis of the Project Fire II Afterbody Flow. *Journal of Thermophysics and Heat Transfer - J THERMOPHYS HEAT TRANSFER*. 17. 240-249. 10.2514/2.6757
- [3]. Olejniczak, J., Prabhu, D., Wright, M., & Bose, D. (2004). *Aeroheating Analysis for the Afterbody of a Titan Probe*. 42nd AIAA Aerospace Sciences Meeting and Exhibit. doi:10.2514/6.2004-486
- [4]. Sinha, K., Barnhardt, M., and Candler, G.V. "Detached Eddy Simulation of Hypersonic Base Flows with Application to Fire II Experiments". AIAA Paper, 2004-2633, 2004.
- [5]. Nalluri, Likhith & Bangi, Vijaya Krishna Teja & Shaik, Mohamed Nizamuddin. (2018). CFD analysis of Reentry Space Shuttle.
- [6]. Bruce Ralphin Rose. J, Saranya. P, "High Temperature Flow Characteristics over a Re-Entry Space Vehicle", *International Journal of Latest Trends in Engineering and Technology (IJLTET)*
- [7]. U, SHIVA & G, Srinivas. (2012). Flow Simulation over Re-Entry Bodies at Supersonic & Hypersonic Speeds. *International Journal of Engineering Research & Development*. 2. 29-34.
- [8]. Christopher J. Roy and Frederick G. Blottner, Assessment of One- and Two-Equation Turbulence Models for Hypersonic Transitional Flows, *Journal Of Spacecraft and Rockets*, Vol. 38, No. 5, September–October 2001
- [9]. Hirschel, E.H., Basics of Aerothermodynamics, progress in Astronautics and Aeronautics, AIAA, Reston, Vol.204. Springer,2004.
- [10]. Roop N. Gupta, Jim J. Jones, and William C. Rochelle, Stagnation-Point Heat-Transfer Rate Predictions at Aeroassist Flight Conditions, NASA TP-3208, NASA-Langley, 1992.